SPEKTRA: Jurnal Fisika dan Aplikasinya
Volume 10, Issue 1, April 2025
Homepage: doi.org/10.21009/SPEKTRA

DOI: doi.org/10.21009/SPEKTRA.101.03

Enhanced Optical Properties of Ce-Doped ZnO Nanoparticles via A Green Plant-Based Synthesis Approach

Mediniah Putri Simatupang, Ari Sulistyo Rini*, Erwin

Department of Physics, Faculty of Mathematics and Natural Sciences, University of Riau, Pekanbaru, 28293, Indonesia

*Corresponding Author Email: ari.sulistyo@lecturer.unri.ac.id

Received: 13 December 2024
Revised: 22 January 2024
Accepted: 11 February 2025
Online: 15 April 2025
Published: 30 April 2025

SPEKTRA: Jurnal Fisika dan Aplikasinya
p-ISSN: 2541-3384
e-ISSN: 2541-3392

ABSTRACT

This study investigated the optical properties of Ce-doped ZnO nanoparticles (Ce/ZnO), synthesized using *Pandanus ammaryllifolius* leaf extract via a green biosynthesis method. Ce doping concentrations of 1%, 2%, and 3% were applied, and the nanoparticles were annealed at 400 °C for two hours. UV-Vis analysis showed a redshift in the annealed samples, with the wavelength increasing from 368 nm to 370 nm, likely due to particle growth after thermal treatment. In contrast, the unannealed samples exhibited a blueshift, with the maximum absorbance wavelength decreasing from 361 nm to 356 nm. The absorbance values were higher in the annealed samples than in the unannealed ones. The band gap energy of doped ZnO samples decreased slightly after annealing, from 3.20–3.22 eV to 3.15–3.19 eV, indicating improved optical properties. FTIR analysis revealed the presence of Ce–O bonds and functional groups, such as O–H and C–H, with sharper peaks in the annealed samples. The novelty of this study lies in utilizing Pandanus ammaryllifolius leaf extract as a natural reducing and stabilizing agent, providing a sustainable and eco-friendly alternative to conventional chemical synthesis methods. The findings suggest that Ce doping enhances the optical properties of ZnO nanoparticles, making them suitable for specific applications in environmental remediation, such as the degradation of organic pollutants, and in technological fields like photocatalytic devices and UV-absorbing materials.

Keywords: biosynthesis, Ce doped ZnO, optical properties, *Pandanus ammaryllifolius*

INTRODUCTION

Zinc oxide (ZnO) nanoparticles are widely recognized for their remarkable optical properties, including a wide bandgap of approximately 3.37 eV and strong ultraviolet absorption. These properties make ZnO a promising material for various optical applications, such as UV-blocking agents, optoelectronics, and photocatalysis [1]. By doping ZnO with rare earth elements like cerium (Ce), its optical behavior can be further tailored to improve light absorption and enhance the material's performance [2]. Ce doping introduces defect levels in the band structure of ZnO, which can reduce the bandgap and shift the optical absorption toward the visible spectrum, making it highly useful for energy and environmental applications [3].

Despite the advancements in ZnO nanoparticle synthesis, significant challenges remain in optimizing their optical properties for specific applications. Conventional chemical methods often involve toxic chemicals and energy-intensive processes, which raise environmental and economic concerns [4]. Biosynthesis, an emerging green synthesis method, addresses these limitations by offering a sustainable and eco-friendly alternative. However, few studies are currently exploring the optimization of biosynthesized ZnO nanoparticles' optical properties through controlled doping and post-synthesis treatments such as annealing. This study aims to fill this gap by investigating the effects of Ce doping concentrations and annealing processes on the optical behavior of ZnO nanoparticles [2], [5].

Biosynthesis involves using biological resources, such as plant extracts, as reducing and stabilizing agents [6]. This approach has gained popularity due to its eco-friendly nature, cost-effectiveness, and ability to produce nanoparticles with superior optical properties. The bioactive compounds in plant extracts, including flavonoids and phenolics, play a crucial role in reducing metal ions and controlling the size and shape of the resulting nanoparticles [7]. For example, extracts from green tea (*Camellia sinensis*), tulsi (*Ocimum tenuiflorum*), and aloe vera (*Aloe barbadensis*) have been widely reported to aid in nanoparticle synthesis due to their rich content of polyphenols, terpenoids, and other antioxidants. However, the effectiveness of different plant extracts varies significantly depending on their unique phytochemical compositions [8]–[10].

The use of *Pandanus amaryllifolius* (Pandan) leaf extract in the biosynthesis of nanoparticles offers distinct advantages. Pandan extract is rich in antioxidants and natural reducing agents that promote nanoparticle formation under mild conditions [11]. Its phytochemical profile, which includes specific phenolic compounds, distinguishes it from other plant extracts commonly used in biosynthesis. Compared to other extracts, such as those from green tea or neem, Pandan leaf extract provides enhanced stability and tunability of the optical properties of synthesized nanoparticles, making it a valuable candidate for green synthesis [12]. Furthermore, the ability of Pandan extract to influence UV-Vis absorption and enhance the optical performance of Ce-doped ZnO nanoparticles highlights its potential for applications in photocatalysis, optical sensors, and environmental remediation [9].

This paper analyzes the optical properties of Ce-doped ZnO nanoparticles synthesized using Pandanus amaryllifolius leaf extract. The main objectives are to investigate the effect of

different cerium doping concentrations on the absorbance and bandgap energy of the nanoparticles, to explore the unique role of Pandan extract in influencing these optical properties, and to assess the impact of annealing on the nanoparticles' optical behavior. The nanoparticles were characterized using ultraviolet-visible (UV-Vis) spectroscopy to measure absorbance and estimate bandgap energy, and Fourier-transform infrared (FTIR) spectroscopy to identify functional groups and examine structural changes. This study highlights the practicality of biosynthesized Ce-doped ZnO nanoparticles for functional and environmental applications by addressing the existing research gaps.

METHOD

The extract of Pandan leaves was utilized as a bioreactor for the synthesis of Ce-doped ZnO nanoparticles. The extraction process involved washing, cutting, and drying the leaves under direct sunlight until fully dry. The extract was prepared by mixing 10 grams of dried Pandan leaves with 200 mL of distilled water and stirring the mixture for 1 hour. The pH of the extract was maintained at 7.0 using a pH meter, and the extraction process was performed at a temperature of 50°C to preserve the bioactive compounds in the leaves. To synthesize of Ce/ZnO nanoparticles, 20 mL of Pandan leaf extract was mixed with 0.05 M $Zn(NO_3)_2.6H_2O$ (HIMEDIA®) and 0.05 M $Ce(NO_3)_3.6H_2O$ (LOBA CHEMIE 99.9%) solution. The mixture was then microwaved for 5 minutes at 540 W. The microwave method was chosen to ensure rapid and uniform heating, which promotes nanoparticle formation while preventing agglomeration. Subsequently, the solution was centrifuged at 2000 rpm for 10 minutes to separate the residue, which was then dried at 110°C. This drying process resulted in the formation of Ce/ZnO nanoparticles, which were further annealed at 400°C for 2 hours to enhance their optical properties. The annealing temperature of 400°C and duration of 2 hours were selected based on the thermal stability and crystallization temperature range of ZnO, ensuring optimal structural and optical improvements [13]. The optical properties and functional groups of the Ce/ZnO nanoparticles were examined using UV-Vis spectroscopy (Agilent Cary 60) and FTIR spectroscopy (Shimadzu IR Prestige-21). Both instruments were calibrated before use to ensure accurate measurements. The UV-Vis spectrophotometer was calibrated with a baseline correction using distilled water as the reference. For the FTIR analysis, the system was calibrated using a standard polystyrene film to verify the accuracy of wavenumber readings [14], [15].

RESULTS AND DISCUSSION

Optical Analysis

The optical properties of Ce-doped ZnO nanoparticles were characterized using UV-Vis spectroscopy, focusing on the absorbance within the 340–400 nm wavelength range. Strong absorbance was observed in this range, typical for ZnO nanoparticles [16]. As shown in TABLE 1, the absorbance analysis provided insight into how Ce doping affected the optical properties under both annealed and unannealed conditions. FIGURE 1 and FIGURE 2

illustrate the absorbance spectra, band gap energy values, and key trends for each doping level [17].

In the unannealed samples, a clear blueshift occurs as the Ce doping concentration increases, with the maximum absorbance shifting to shorter wavelengths of 361 nm, 358 nm, and 356 nm for 1%, 2%, and 3% Ce doping, respectively. Thus, the absorbance value decreases from 0.27 at 1% to 0.11 at 3%. The band gap energy increases slightly from 3.20 eV to 3.22 eV as the doping concentration increases. This shift can be attributed to the quantum confinement effect, where a smaller particle size increases the band gap energy, pushing the absorbance to shorter wavelengths [18]. The blueshift is also associated with localized energy levels introduced by Ce ions, which enhance electron-hole recombination and alter optical transitions within the ZnO lattice [19].

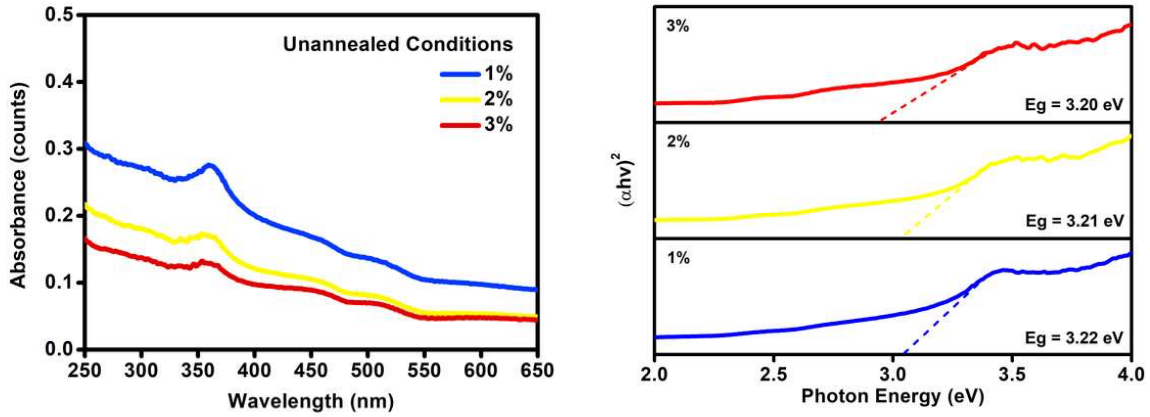

(a) (b)

FIGURE 1. Absorbance spectra of unannealed Ce-doped ZnO nanoparticles. The graph highlights the blueshift in absorbance peaks and the corresponding increase in band gap energy with increasing Ce doping concentrations. These trends are attributed to the quantum confinement effect.

After annealing at 400 °C, the optical properties exhibit a redshift, with peak absorbance shifting to longer wavelengths of 368 nm, 369 nm, and 370 nm for 1%, 2%, and 3% Ce doping, respectively. The overall absorbance also increases, especially for the 1% Ce-doped sample, which shows a peak value of 0.39. The band gap energy decreases slightly to 3.15 eV, 3.17 eV, and 3.19 eV for each doping level. This redshift is explained by the increased particle size and enhanced crystallinity due to the annealing process [13]. Annealing allows Ce ions to integrate more effectively into the ZnO matrix, reducing oxygen vacancies and suppressing non-radiative recombination, thereby improving optical performance [18]. These findings align with prior studies that reported similar trends in doped ZnO systems. For instance, the Er-doped ZnO sample demonstrated a reduction in the reflection band and a redshift, which was attributed to the creation of faulty energy levels within the energy bands around the Fermi level or oxygen deficiency [20]. Similarly, the absorbance spectrum of Se-doped ZnO exhibited a redshift due to single oxygen vacancies caused by electron-hole radiation at the oxygen vacancy sites [21]. Conversely, increasing Se concentration in ZnO led to a blueshift in the absorption peak, indicating a quantum confinement effect due to interactions between ZnO and Se [22]. The blue and red shifts observed in these studies are consistent with the

effects of quantum confinement, particle growth, and structural modifications. This comparison highlights the novelty of using Ce doping and annealing to fine-tune the optical properties of ZnO [2], [23].

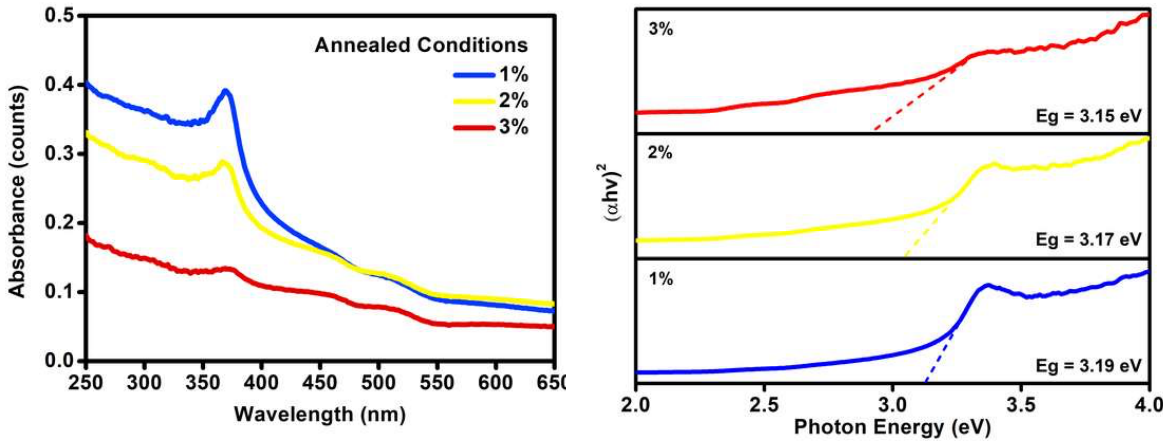

(a) (b)

FIGURE 2. Absorbance spectra of annealed Ce-doped ZnO nanoparticles at 400 °C. The figure illustrates the redshift in absorbance peaks and the decrease in band gap energy due to particle growth and improved crystallinity. The annealing process enhances optical properties by reducing oxygen vacancies and non-radiative recombination.

In this study, "redshift" and "blueshift" describe the directional changes in the absorbance peak wavelength, as summarized in TABLE 1. These terminologies provide an intuitive understanding of the optical changes induced by Ce doping and annealing. The combination of Ce doping and annealing demonstrates the tunability of ZnO's optical properties, which can be further optimized for applications in photocatalysis and optoelectronics [24].

TABLE 1. Comparison of absorbance and energy gap values in annealed and unannealed samples.

Condition	Sample	Wavelength (nm)	Absorbance (a.u)	Band Gap Energy (Ev)
Unannealed	1%	361	0.27	3.20
	2%	358	0.17	3.21
	3%	356	0.11	3.22
Annealed	1%	368	0.39	3.15
	2%	369	0.28	3.17
	3%	370	0.14	3.19

Functional Group Analysis

The functional groups of the Ce-doped ZnO nanoparticles were identified through FTIR spectroscopy, which is essential for understanding the chemical interactions and surface modifications resulting from both the synthesis and doping processes [25]. FIGURE 3(a) and FIGURE 3(b) display the FTIR spectra for unannealed and annealed samples, highlighting significant changes in functional groups due to thermal treatment [26].

In unannealed samples, broad peaks at 3500–3000 cm^{-1} correspond to O–H stretching vibrations, indicating the presence of surface hydroxyl groups adsorbed during biosynthesis. Peaks at 2920–2850 cm^{-1} represent C–H stretching vibrations from organic residues in the Pandanus leaf extract, while bands at 1650–1550 cm^{-1} suggest N–H bending vibrations, likely originating from biomolecules in the extract. The 1400–1200 cm^{-1} range exhibits peaks for C=O stretching vibrations, which are known to stabilize nanoparticles in green synthesis processes [27]–[29]. The 500–600 cm^{-1} peak is also attributed to Ce–O bond formation, confirming successful Ce doping. However, the unannealed samples retain significant organic residues and exhibit less-defined bonding due to incomplete crystallization [30].

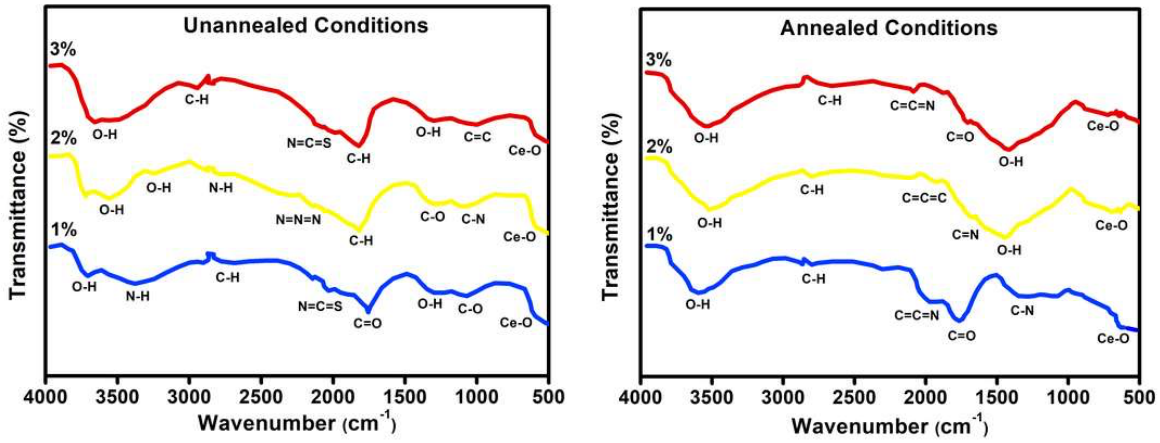

(a) (b)

FIGURE 3. (a) FTIR spectra of unannealed Ce-doped ZnO nanoparticles, revealing functional groups from biosynthesis and Ce doping, with peaks indicating hydroxyl, amine, and Ce–O bonds. (b) FTIR spectra of annealed Ce-doped ZnO nanoparticles, showing reduced organic residues and prominent Ce–O bonding, indicating enhanced crystallinity and structural stability.

After annealing at 400 °C, the O–H stretching peak diminishes, reflecting the removal of surface hydroxyl groups and moisture. C–H stretching peaks become sharper, indicating reduced organic residue content, while the N–H bending and C=O stretching bands weaken, suggesting fewer amine and carbonyl groups. Most notably, the Ce–O peak becomes more prominent and well-defined after annealing, signifying enhanced Ce incorporation into the ZnO lattice and improved crystallinity. These observations align with previous studies that reported enhanced structural and chemical stability in annealed doped ZnO nanoparticles [28]. Previous studies have demonstrated that annealing processes significantly affect the structural and optical properties of materials. For instance, annealing at various temperature ranges under a vacuum condition of 4.5×10^{-6} Torr reduced reflectance by 13–11% due to plasmonic effects, enhancing the solar cell conversion efficiency [31]. Additionally, it has been shown that the morphology, structure, and annealing temperature of ZnO influences the surface-to-bulk ratio, surface area, and surface activity, which, in turn, affect the photodegradation rate of organic dyes [32]–[34]. A study achieved 98.8% degradation efficiency by doping ZnO with 1% Sn, with the improvement attributed to changes in structural, optical, and electrical properties [35]. The C–H stretching peaks at 2920–2850 cm^{-1} become sharper and more

defined, reflecting the removal of loosely bound organic matter and the possible stabilization of residual functional groups. The N–H bending peak at 1650 cm^{-1} decreases, suggesting a reduction in amine content, while C=O stretching bands remain visible but less intense [29]. Most importantly, the Ce–O bond around 500–600 cm^{-1} becomes more prominent and well-defined after annealing, which points to enhanced cerium incorporation into the ZnO matrix. This improvement indicates better crystallinity and integration of Ce ions within the ZnO structure [23]. Annealing likely contributes to the removal of surface defects and organic residues, promoting a more stable and crystalline nanoparticle structure, thereby enhancing optical properties [36].

In this study, similar trends were observed, where annealing at 400 °C reduced surface hydroxyl groups (O–H) and organic residues, as indicated by the weakening of N–H bending and C=O stretching peaks, alongside the sharpening of C–H stretching peaks. Most notably, the Ce–O peak became more prominent, signifying enhanced cerium incorporation into the ZnO lattice and improved crystallinity. These findings are consistent with previous reports, which noted enhanced structural and chemical stability in annealed doped ZnO [30]. Annealing also eliminates surface defects and organic residues, improving optical properties by reducing electron-hole recombination and enabling better band gap tunability through structural refinement [37]. This highlights that Ce doping, in combination with annealing, is an effective strategy for improving the performance of photocatalytic materials, particularly in the degradation of organic pollutants [33].

CONCLUSION

To summarize, Ce doping in ZnO nanoparticles significantly alters their optical and structural properties, making them suitable for advanced applications such as photocatalysis. UV-Vis analysis revealed a blueshift in unannealed samples (361 to 356 nm) and a redshift after annealing (368 to 370 nm), accompanied by a decrease in band gap energy post-annealing (3.20 eV to 3.19 eV), indicating enhanced light absorption and potential for increased photocatalytic activity. FTIR spectra confirmed the presence of critical functional groups with stronger Ce–O bonds and reduced surface hydroxyls after annealing, reflecting better structural integration and crystallinity. These improvements suggest that Ce-doped ZnO nanoparticles can be efficiently utilized in environmental and catalytic applications, such as pollutant degradation. However, challenges such as optimizing doping concentrations and scalability for industrial use remain. Future studies should address these limitations, explore different doping elements, and test the material's performance in real-world environmental conditions. The methodology developed in this study could serve as a foundation for further exploration of doped ZnO-based photocatalysts, advancing the scientific understanding and practical application of these materials.

ACKNOWLEDGMENTS

Indonesia's Ministry of Education, Culture, Research, and Technology financially supported this project through a Master's Thesis Research Grant in 2024. The authors sincerely thank

the Research and Community Service Institute (LPPM) at the University of Riau for their continuous support.

REFERENCES

[1] K. K. Supin, P. N. Parvathy Namboothiri, and M. Vasundhara, "Enhanced photocatalytic activity in ZnO nanoparticles developed using novel *Lepidagathis ananthapuramensis* leaf extract," *RSC Adv.*, vol. 13, no. 3, pp. 1497–1515, 2023, doi: 10.1039/d2ra06967a.

[2] S. Kim, M. Choi, and J. Park, "Cerium-Doped Oxide-Based Materials for Energy and Environmental Applications," *Crystals*, vol. 13, no. 12, 2023, doi: 10.3390/cryst13121631.

[3] C. de M. Strieder, D. L. P. Macuvele, C. Soares, N. Padoin, and H. G. Riella, "Plant-mediated green synthesis of cerium oxide nanoparticles: A critical perspective of some unclear issues," *J. Mater. Res. Technol.*, vol. 30, pp. 6376–6388, 2024, doi: 10.1016/j.jmrt.2024.05.022.

[4] I. Usman et al., "Traditional and innovative approaches for extracting bioactive compounds," *Int. J. Food Prop.*, vol. 25, no. 1, pp. 1215–1233, 2022, doi: 10.1080/10942912.2022.2074030.

[5] N. Yadav, "Cerium oxide nanostructures: Properties, biomedical applications, and surface coatings," *3 Biotech*, vol. 12, no. 5, pp. 1–20, 2022, doi: 10.1007/s13205-022-03186-3.

[6] M. A. Fagier, "Plant-Mediated Biosynthesis and Photocatalysis Activities of Zinc Oxide Nanoparticles: A Prospect towards Dyes Mineralization," *J. Nanotechnol.*, vol. 2021, 2021, doi: 10.1155/2021/6629180.

[7] R. Rajamani et al., "Mitigating global challenges: Harnessing green synthesized nanomaterials for sustainable crop production systems," *Glob. Challenges*, vol. 8, no. 1, pp. 1–15, 2024, doi: 10.1002/gch2.202300187.

[8] A. Wirwis and Z. Sadowski, "Green synthesis of silver nanoparticles: Optimizing green tea leaf extraction for enhanced physicochemical properties," *ACS Omega*, vol. 8, no. 33, pp. 30532–30549, 2023, doi: 10.1021/acsomega.3c03775.

[9] R. F. Rumana et al., "Tulsi mediated green synthesis of zinc doped CeO_2 for supercapacitor and display applications," *J. Sci. Adv. Mater. Devices*, vol. 8, no. 2, p. 100551, 2023, doi: 10.1016/j.jsamd.2023.100551.

[10] Y. Song et al., "Green synthesized Se–ZnO/attapulgite nanocomposites using *Aloe vera* leaf extract: Characterization, antibacterial and antioxidant activities," *Lwt*, vol. 165, p. 113762, 2022, doi: 10.1016/j.lwt.2022.113762.

[11] R. M. Akhir et al., "The potential of *Pandanus amaryllifolius* leaves extract in the fabrication of dense and uniform ZnO microrods," *Micromachines*, vol. 11, no. 3, pp. 1–14, 2020, doi: 10.3390/mi11030299.

[12] M. Efenberger-Szmechtyk, A. Nowak, and A. Czyzowska, "Plant extracts rich in polyphenols: antibacterial agents and natural preservatives for meat and meat products," *Crit. Rev. Food Sci. Nutr.*, vol. 61, no. 1, pp. 149–178, 2021, doi: 10.1080/10408398.2020.1722060.

[13] R. Fadillah, Y. Rati, R. Dewi, R. Farma, and A. S. Rini, "Optical and structural studies on bio-synthesized ZnO using *Citrullus lanatus* peel extract," *J. Phys. Conf. Ser.*, vol. 1816, no. 1, 2021, doi: 10.1088/1742-6596/1816/1/012019.

[14] Y. Guo, C. Liu, R. Ye, and Q. Duan, "Advances on water quality detection by UV-Vis spectroscopy," *Appl. Sci.*, vol. 10, no. 19, pp. 1–18, 2020, doi: 10.3390/app10196874.

[15] M. O. Yusuf, "Bond characterization in cementitious material binders using Fourier-transform infrared spectroscopy," *Appl. Sci.*, vol. 13, no. 5, 2023, doi: 10.3390/app13053353.

[16] Z. S. Amin et al., "Synthesis, characterization and biological activities of zinc oxide nanoparticles derived from secondary metabolites of *Lentinula edodes*," *Molecules*, vol. 28, no. 8, pp. 1–17, 2023, doi: 10.3390/molecules28083532.

[17] A. Shulga, L. A. Butusov, G. K. Chudinova, and T. F. Sheshko, "Microwave-assisted synthesis of cerium doped ZnO nanostructures and its optical properties," *J. Phys. Conf. Ser.*, vol. 1461, no. 1, 2020, doi: 10.1088/1742-6596/1461/1/012162.

[18] Z. Ait Abdelouhab, D. Djouadi, A. Chelouche, L. Hammiche, and T. Touam, "Structural and morphological characterizations of pure and Ce-doped ZnO nanorods hydrothermally

synthesized with different caustic bases," *Mater. Sci. Pol.*, vol. 38, no. 2, pp. 228–235, 2020, doi: 10.2478/msp-2020-0038.

[19] I. Y. Habib, N. M. Zain, C. M. Lim, A. Usman, N. T. R. N. Kumara, and A. H. Mahadi, "Effect of doping rare-earth element on the structural, morphological, optical and photocatalytic properties of ZnO nanoparticles in the degradation of methylene blue dye," *IOP Conf. Ser. Mater. Sci. Eng.*, vol. 1127, no. 1, p. 012004, 2021, doi: 10.1088/1757-899X/1127/1/012004.

[20] M. C. R. Silva et al., "Green synthesis of Er-doped ZnO nanoparticles: An investigation on the methylene blue, eosin, and ibuprofen removal by photodegradation," *Molecules*, vol. 29, no. 2, 2024, doi: 10.3390/molecules29020391.

[21] A. S. Rini, A. H. Sitorus, M. P. Simatupang, E. Taer, Z. Usman, and Jasril, "Influence of sulfur addition on the physical and photocatalytic properties biosynthesized Se-doped ZnO nanoparticles," *J. Phys. Conf. Ser.*, 2024, doi: 10.1088/1742-6596/2866/1/012005.

[22] A. S. Rini, M. P. Simatupang, Y. Rati, and R. Dewi, "Matoa leaf extract mediated synthesis of Se-doped ZnO nanoparticles and their photocatalytic capability," *Process. Appl. Ceram.*, vol. 18, no. 1, pp. 12–19, 2024, doi: 10.2298/PAC2401012R.

[23] S. Karidas, B. K. Veena, N. Pujari, P. Krishna, and V. Chunduru, "Photodegradation of methylene blue (MB) using cerium-doped zinc oxide nanoparticles," *Sadhana - Acad. Proc. Eng. Sci.*, vol. 45, no. 1, 2020, doi: 10.1007/s12046-020-01329-x.

[24] B. T. Phan, T. U. Doan Thi, T. T. Nguyen, Y. D. Thi, K. H. Ta Thi, and K. N. Pham, "Green synthesis of ZnO nanoparticles using orange fruit peel extract for antibacterial activities," *RSC Adv.*, vol. 10, no. 40, pp. 23899–23907, 2020, doi: 10.1039/d0ra04926c.

[25] I. Ilahi et al., "Synthesis of silver nanoparticles using root extract of *Duchesnea indica* and assessment of its biological activities," *Arab. J. Chem.*, vol. 14, no. 5, p. 103110, 2021, doi: 10.1016/j.arabjc.2021.103110.

[26] R. D. Kaushik, S. Kumar, S. K. Sharma, and L. P. Purohit, "Chalcogen-doped zinc oxide nanoparticles for photocatalytic degradation of Rhodamine B under the irradiation of ultraviolet light," *Mater. Today Chem.*, vol. 20, p. 100464, 2021, doi: 10.1016/j.mtchem.2021.100464.

[27] A. S. Rini, Y. Rati, and S. W. Maisita, "Synthesis of ZnO nanoparticles using *Sandoricum koetjape* peel extract as bio-stabilizer under microwave irradiation," *J. Phys. Conf. Ser.*, vol. 2049, no. 1, 2021, doi: 10.1088/1742-6596/2049/1/012069.

[28] R. M. Salim, J. Asik, and M. S. Sarjadi, "Chemical functional groups of extractives, cellulose and lignin extracted from native *Leucaena leucocephala* bark," *Wood Sci. Technol.*, vol. 55, no. 2, pp. 295–313, 2021, doi: 10.1007/s00226-020-01258-2.

[29] A. Can and K. Kizilbey, "Green synthesis of ZnO nanoparticles via *Ganoderma lucidum*," *Gels*, vol. 10, no. 576, 2024.

[30] T. Bouarroudj et al., "Enhanced photocatalytic activity of Ce and Ag co-doped ZnO nanorods for paracetamol and metronidazole antibiotics co-degradation in wastewater promoted by solar light," *Russ. J. Phys. Chem. A*, vol. 97, no. 5, pp. 1074–1087, 2023, doi: 10.1134/S0036024423050278.

[31] A. Singh and K. Kaur, "Biological and physical applications of silver nanoparticles with emerging trends of green synthesis," *Eng. Nanomater. - Health Saf.*, 2020, doi: 10.5772/intechopen.88684.

[32] T. Al-Garni, N. A. Y. Abduh, A. Al-Kahtani, and A. Aouissi, "Synthesis of ZnO nanoparticles by using *Rosmarinus officinalis* extract and their application for methylene blue and crystal violet dyes degradation under sunlight irradiation," *Preprints*, no. April, p. 2021040038, 2021, doi: 10.20944/preprints202104.0038.v1.

[33] N. Q. Yang, J. Li, Y. N. Wang, and J. Ma, "Investigation of photocatalytic properties based on Fe and Ce co-doped ZnO via the hydrothermal method and first principles," *Mater. Sci. Semicond. Process.*, vol. 131, no. April, p. 105835, 2021, doi: 10.1016/j.mssp.2021.105835.

[34] K. K. Taha, M. M. Mustafa, H. A. M. Ahmed, and S. Talab, "Selenium zinc oxide (Se/ZnO) nanoparticles: Synthesis, characterization, and photocatalytic activity," *Zeitschrift für Naturforsch. - Sect. A J. Phys. Sci.*, 2019, doi: 10.1515/zna-2019-0157.

[35] R. Beura, R. Pachaiappan, and P. Thangadurai, "A detailed study on Sn^{4+} doped ZnO for enhanced photocatalytic degradation," *Appl. Surf. Sci.*, vol. 433, pp. 887–898, 2018, doi: 10.1016/j.apsusc.2017.10.127.

[36] A. G. Kaningini et al., "Effect of optimized precursor concentration, temperature, and doping on optical properties of ZnO nanoparticles synthesized via a green route using bush tea (*Athrixia phylicoides* DC.) leaf extracts," *ACS Omega*, vol. 7, no. 36, pp. 31658–31666, 2022, doi: 10.1021/acsomega.2c00530.

[37] L. Zhang, M. Golmohammadi, and M. N. Hassankiadeh, "Facile biosynthesis of SnO_2/ZnO nanocomposite using *Acroptilon repens* flower extract and evaluation of their photocatalytic activity," *Ceram. Int.*, vol. 47, no. 20, pp. 29303–29308, 2021, doi: 10.1016/j.ceramint.2021.07.095.